[redacted] LA-UR-98-3655
CONF-980827--

Title: BEAM DYNAMICS SIMULATION OF THE SPALLATION NEUTRON SOURCE LINEAR ACCLERATOR

Author(s): Harunori Takeda, LANSCE-1
James H. Billen, LANSCE-1
Tarlochan Bhatia, LANSCE-1

Submitted To: LINAC '98
XIX INTERNATIONAL CONFERENCE
CHICAGO, IL AUGUST 23-28, 1998

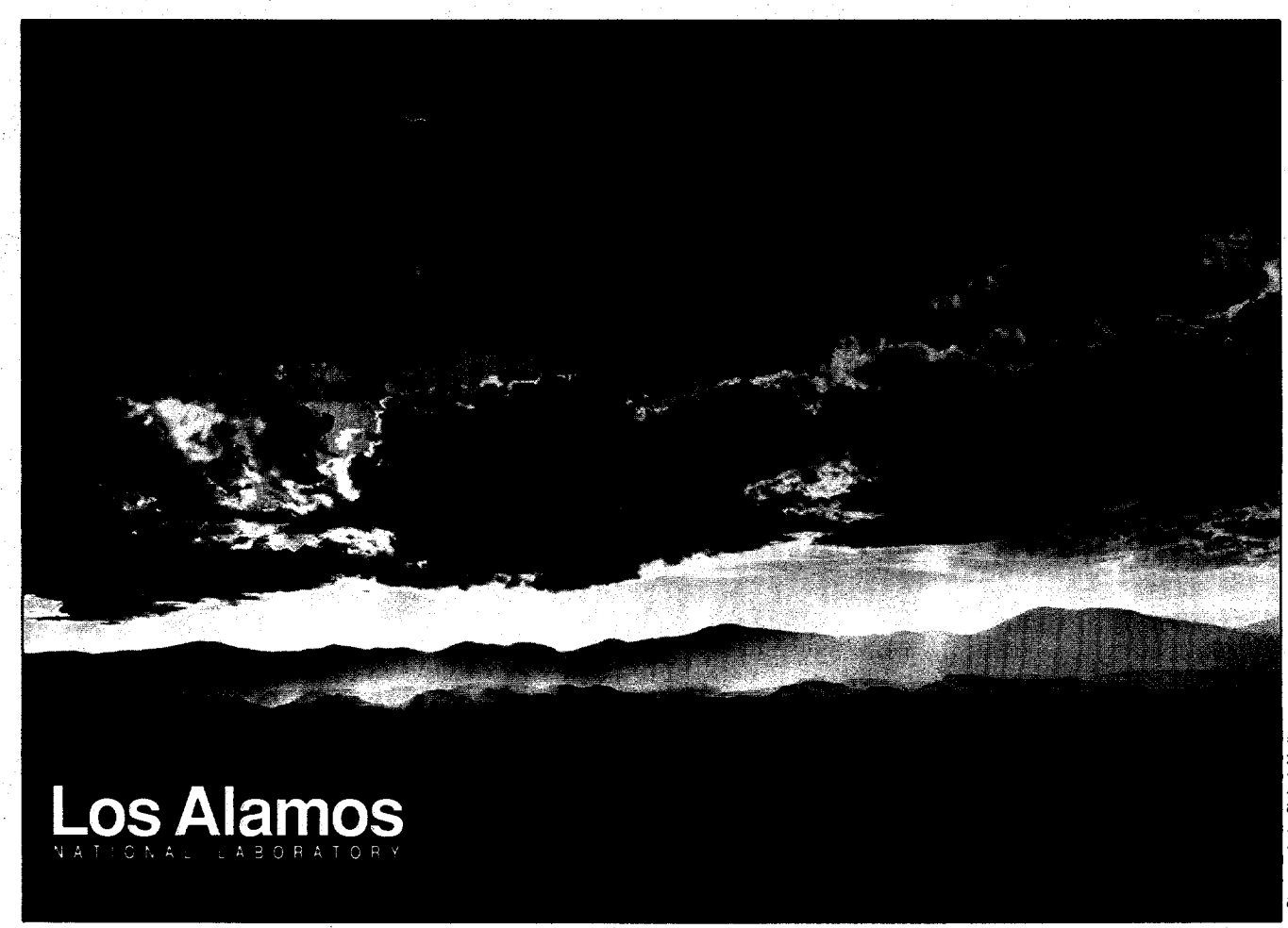

DISCLAIMER

BEAM DYNAMICS SIMULATION OF THE SPALLATION NEUTRON SOURCE LINAEAR ACCELERATOR*

H. Takeda, J. H. Billen, T. S. Bhatia
Los Alamos National Laboratory, Los Alamos, New Mexico 87545 USA

Abstract

The accelerating structure for Spallation Neutron Source (SNS) consists of a radio-frequency-quadrupole-linac (RFQ), a drift-tube-linac (DTL), a coupled-cavity-drift-tube-linac (CCDTL) [1], and a coupled-cavity-linac (CCL). The linac is operated at room temperature. We discuss the detailed design of linac which accelerates an H^- pulsed beam coming out from RFQ at 2.5 MeV to 1000 MeV. We show a detailed transition from 402.5 MHz DTL with a 4 $\beta\lambda$ structure to a CCDTL operated at 805 MHz with a 12 $\beta\lambda$ structure. After a discussion of overall feature of the linac, we present an end-to-end particle simulation using the new version of the PARMILA code [2] for a beam starting from the RFQ entrance through the rest of the linac. At 1000 MeV, the beam is transported to a storage ring. The storage ring requires a large (±500-keV) energy spread. This is accomplished by operating the rf-phase in the last section of the linac so the particles are at the unstable fixed point of the separatrix. We present zero-current phase advance, beam size, and beam emittance along the entire linac.

1. LINAC STRUCTURES

We consider the DTL, CCDTL and two types of CCL part of linac structure. At the linac structure change between structures, we apply discontinuous accelerating electric fields between structures to maintain a continuous real-estate phase advance per unit length. The design phase was made continuous at the structure junctions to avoid the abrupt longitudinal separatrix change. The DTL with focusing lattice FOFODO structure accelerates the 2.5-MeV H^- beam from the RFQ to 20 MeV. Between the RFQ and the DTL, we have a symmetric beam chopper section which consists of a number of quadrupoles and three buncher cavities.

The CCDTL then takes the beam from the DTL and accelerates it to 94 MeV. To match the beam from the DTL to the CCDTL, we use the first two cavities (4 cells) of the CCDTL operating at –90° and adjust the first four quadrupole magnet strengths. Each cavity in the CCDTL contains a drift tube. A focusing (or defocusing) quadrupole magnet follows every two CCDTL cavities. In the DTL the transverse lattice is of type FOFODODO with a 4 $\beta\lambda$ period at 402.5 MHz. Starting in the CCDTL the transverse lattice changes to FODO with a 12 $\beta\lambda$ period at 805 MHz. The term FODO (pronounced "foe-doe") refers to singlet quadrupole magnets arranged in an alternating gradient focusing system. The letter O was originally a numeral zero, and indicates a drift space between a focusing magnet F and a defocusing magnet D.

Above about 95 MeV the efficiency of a conventional CCL exceeds that of the CCDTL. The 805-MHz CCL continues the 12 $\beta\lambda$ periodic transverse lattice of the CCDTL. The first part of CCL consists of 8-cavity segments separated by singlet quadrupole magnets and accelerates the beam to 165 MeV. Above 165 MeV, the CCL consists of 10-cavity segments and completes the acceleration to 1000 MeV. The 8-cavity segments are used at lower energy to provide more space for the quadrupole magnets and diagnostic elements. This entire CCL maintains the FODO lattice structure with a transverse period of 12 $\beta\lambda$ [3]. Table 1 shows the linac characteristics. Figure 1 shows the cavity field along the linac. The field is discontinuous, but the "real-estate" longitudinal focusing force which is proportional to E_0T averaged over a transverse focusing period is continuous, where E_0 is the average axial electric field and T is the transit-time factor. Figure 2 shows the design phase along the linac. Figure 3 shows the zero-current phase advance per transverse focusing period through the CCDTL and CCL.

Table 1. Linac characteristics

Linac Type	Energy (MeV)	Length (m)
DTL	2.50 to 20.275	8.712
CCDTL	20.275 to 94.428	68.78
CCL1	94.428 to 164.65	46.24
CCL2	164.65 to 1000.	369.94

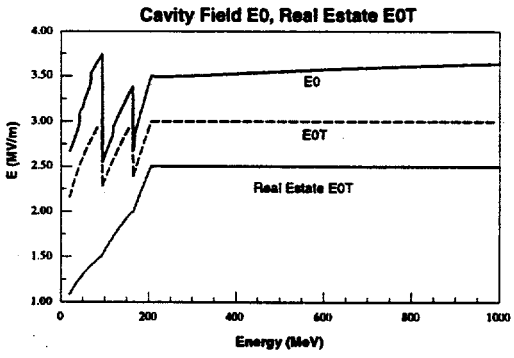

Figure 1. The cavity field E_0 E_0T real estate E_0T from CCDTL to CCL2.

*This work sponsored by the Division of Materials Sciences, US department of Energy, under contract number DE-AC05-96OR22464 with Lockheed Martin Energy Research Corporation for Oak Ridge National Laboratory.

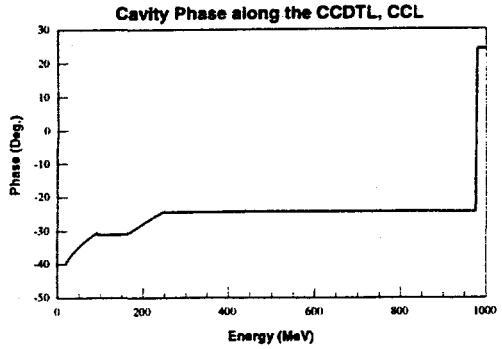

Figure 2. The design phase starting in the CCDTL. The phase change near the end of the CCL from –24 to +24 degrees increases the energy spread as required for ring injection.

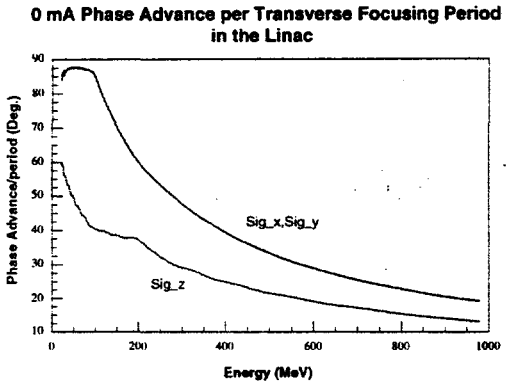

Figure 3. Zero-current phase advance per 12 βλ in the CCDTL and CCL.

2. DTL TO CCDTL TRANSITION

To achieve a smooth beam match between the DTL and the CCDTL, we require that the transverse and longitudinal real-estate phase advances are continuous across the matching section. The longitudinal matching section consists of the first two CCDTL cavities with a total of 4 accelerating gaps operating at –90°. The transverse matching section consists of four quadrupole magnets after the first segment of the CCDTL. The zero-current transverse phase advance at the end of the DTL is 57.35° with a transverse period 4 βλ at 402.5 MHz. The equivalent phase advance at the entry to the CCDTL, which operates at 805 MHz is 86.025° (= 57.35*12/(4*2)). The longitudinal phase advance is 40° over the transverse period 4 βλ. This translates to 60° at the CCDTL entry. Table 2 shows the matching section linac parameters. Figure 4 shows the transverse and longitudinal beam profiles at the matching section performed with the TRACE 3-D code [4].

Table. 2. Matching section parameters at the CCDTL.

Beam Element	Parameters
Drift	13.27 cm
Q between DTL and CCDTL	–2.692 T
Drift	7.0 cm
Q1	+2.161T
Q2	–2.278T
Q3	+2.261T
Q4	–2.199T
First 2 Cavities	1.9529 MV/m. –90°

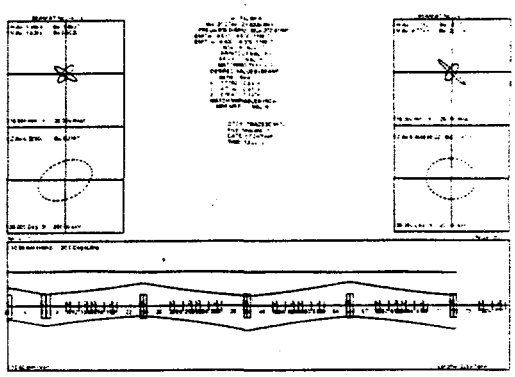

Figure 4. Beam profiles in the first few lattice periods of the CCDTL. This part of the structure is used to match the beam from the DTL.

3. PARMILA SIMULATION FROM DTL TO CCL

Starting at the entry to the DTL with the RFQ exit beam distribution we performed a PARMILA 10,000-particle simulation. The normalized rms emittance was 0.01845 π cm-mr in the transverse phase plane, and 0.1056 π deg-MeV in the longitudinal plane. The beam microbunch current was 55.4 mA. Figure 5 shows the rms beam radius, the maximum radius, and the linac aperture along the linac. It shows that we have sufficient beam clearance along the linac. Figure 6 shows the normalized rms emittances through the linac. The artificial discontinuity in longitudinal emittance at 20 MeV is caused by the doubling of the rf frequency.

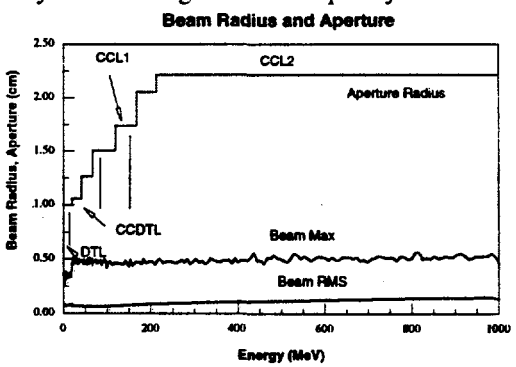

Figure 5. Linac aperture and beam size along the linac.

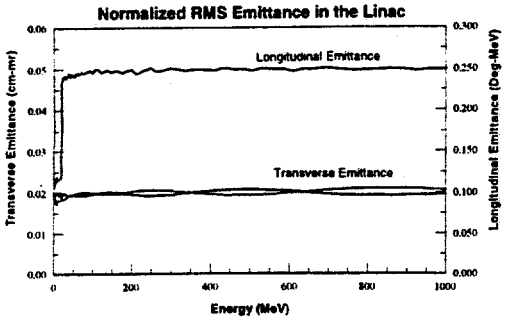

Figure 6. The normalized rms emittances are constant along the linac.

The beam profiles x, y, phase ϕ and energy W through the entire linac from DTL to CCL are plotted in Figure 7. By shifting the rf phase to operate at +24 degrees for the last five 10-cavity segments of the structure, the energy width increases from ±163 keV to ±667 keV.

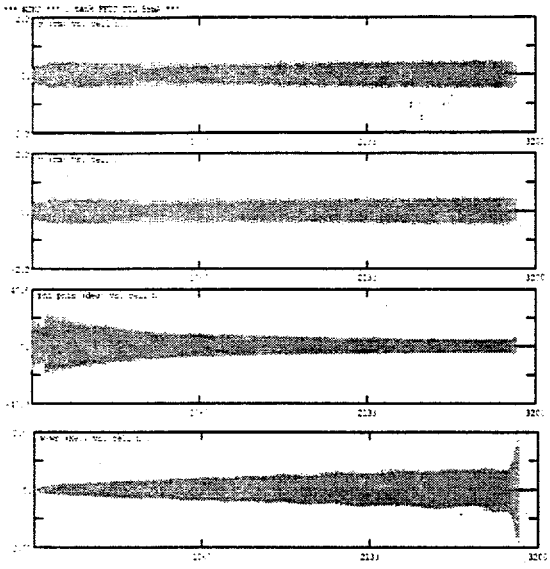

Figure 7. The beam profiles x, y, phase ϕ, and energy W along the linac from DTL. Shifting the rf phase to +24° expands the beam energy width.

4. END-TO-END PARMILA SIMULATION FROM RFQ TO CCL

A 30-mA beam with normalized transverse rms emittance 0.2 π mm-mrad was generated with 4-d waterbag distribution for the RFQ input. The RFQ accelerates the beam to 2.5 MeV. Then a medium-energy beam transport section (MEBT), which houses the chopper and consists of 18 quadrupole magnets and 3 buncher cavities, guides the beam to the DTL. At the entry to the MEBT, the normalized rms beam emittances are 0.206 π mm-mrad transversely and 0.1π MeV-deg longitudinally. Figure 8 shows the x and y beam profiles at the interface between the MEBT and the DTL.

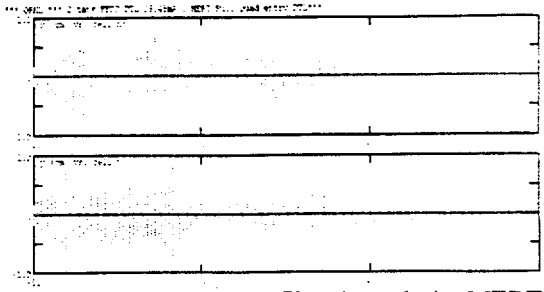

Figure 8. Beam x and y profiles through the MEBT and DTL for a 29.4-mA beam.

Figure 9 shows the x, y, phase, and energy profile of the end-to-end simulation showing from the MEBT through the CCL. The beam starts at the RFQ.

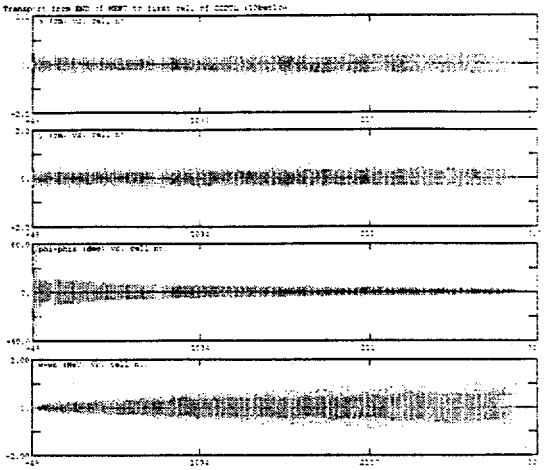

Figure 9. End-to-end simulation for a 29.4-mA beam. The profiles are the same as in Figure 7. The plot shows the profiles starting at the MEBT, but the simulation started at the RFQ entrance.

5. SUMMARY

The PARMILA simulation from the DTL to the end of CCL shows that the beam could be accelerated to 1000 MeV without loss by the sequence of linacs DTL, CCDTL, and CCL.

6. REFERENCES

1 J. H. Billen et al., "A New Rf Structure for Intermediate Velocity Particles," Proceedings of the 1994 Linear Accelerator Conference (August 21-26, 1994 Tsukuba, Japan).

2 H. Takeda and J. H. Billen, "Recent Developments in the Accelerator Design Code PARMILA," this conference.

3 T. S. Bhatia et al., "SNS Linac: Revised Configuration" Los Alamos National Laboratory Report LA-UR-98-3595.

4 K. R. Crandall and D. P. Rusthoi, Trace 3-D Documentation, Los Alamos National Laboratory Report LA-UR-97-886.